Accuracy of SPOT Digital Elevation Model and Derivatives: Utility for Alaska's North Slope

Kathryn Connors Sasowsky
Office for Remote Sensing of Earth Resources, Environmental Resources Research Institute, The Pennsylvania State University, University Park, PA 16802
Gary W. Petersen
Office for Remote Sensing of Earth Resources, Environmental Resources Research Institute, and Agronomy Department, The Pennsylvania State University, University Park, PA 16802
Barry M. Evans
Geo Decisions, Inc., Lemont, PA 16851

ABSTRACT: SPOT (Systeme Probatoire d'Observation de la Terre) data are a valuable source of terrain information, especially for areas of the world which are not covered by large-scale topographic maps. Numerous investigators have developed algorithms to produce digital elevation models (DEMs) from SPOT and have evaluated their accuracy. This investigation not only evaluates the accuracy of a portion of a SPOT DEM but evaluates products derived from it; namely, slopes, aspects, and thickness of thaw layer. A DEM, purchased from STX corporation, was created from an image pair with less than optimum difference between image acquisition angles at a study site in northern Alaska. Root mean square (RMS) errors for elevations were 19.3m and 13.7m and for slopes were 2.7 percent to 4.0 percent. Aspects agree in general slope orientation. Even though the area had relatively low relief (~250m within a ~25km² area), the SPOT-derived DEM provides sufficiently accurate ground elevation, slope gradient, and aspect data for use in ecosystem investigatons. A predictive map of thickness of thaw created from a SPOT-derived DEM was comparable to one created from a very large scale (1:6000) DEM.

INTRODUCTION

LARGE-SCALE topographic maps are not available for many areas of the world. To create these maps, it is necessary to compile stereoscopic imagery and/or survey the land surface. Prior to the launch of the SPOT-1, stereo pairs were provided by overlapping aerial photographs. Generating topographic maps or digital elevation models (DEMs) from satellite data is more automated than producing topographic maps from aerial photographs and less labor intensive than ground surveying. Furthermore, the data are also in a form that can be easily incorporated into a geographic information system (GIS).

Numerous investigators have developed and evaluated algorithms to create DEMs and estimate elevations from SPOT (Arai *et al.*, 1988; Brockelbank and Tam, 1991; Chen *et al.*, 1988; Day and Muller, 1989; Gugan and Dowman, 1988a, 1988b; Forster *et al.*, 1988; Fukushima, 1988; Hanaizumi *et al.*, 1990; Hartley, 1988; Koizumi *et al.*, 1988; Ley, 1988; Millot and Pascand, 1988; Priebbenow and Clerici, 1988; Rodriquez *et al.*, 1988; Rosenholm, 1988; Simard *et al.*, 1988; Swann *et al.*, 1988; Theodossion and Dowman, 1990; Thormodogard and Feuguay, 1988; Veenstra and McMaster, 1988; Vincent *et al.*, 1988). This investigation, therefore, did not focus on these algorithms, but instead, centered on evaluation of a commercially produced SPOT DEM. Details of the algorithm used are not available because software is proprietary. According to STX, the process initially outputs a precision orbit and imagery for which the only differences are due to terrain parallax. Using a series of correlation apertures, whose width and spacing varies with processing stages, the terrain parallax is converted to an elevation measurement (M. Labovitz, personal communication, 1989). Eight control points from survey data were used in the creation of the DEM. No other details of the procedure are available.

Reported elevation accuracies of DEMs from SPOT range from root-mean-square (RMS) errors of 3.4m in low-relief areas with a base-to-height ratio of 1 (Rodriguez *et al.*, 1988), to 101.6m in mountainous areas with a base-to-height ratio of 0.52 (Fukushima, 1988). Elevations have been interpolated to various grid sizes from 10m (Simard *et al.*, 1988; Vincent *et al.*, 1988) to 100m (Dowman, 1988; Ley, 1988) with no consistent relationship between elevation accuracies and grid cell size. Factors such as base-to-height ratios of the original stereoscopic SPOT images, the quality of the images (e.g., amount of cloud cover), terrain relief, availability of control points, and algorithm design affect elevation accuracy of DEMs created from SPOT. Higher base-to-height ratios and more control points generally yield more accurate elevation measurements (Gugan and Dowman, 1988).

DEMs created from SPOT may be useful sources of topographic maps or digital elevations at scales of 1:24,000 to 1:50,000 based on reported accuracies (Cooper *et al.*, 1987; Westin, 1988; Wilson and Robertson, 1990). A key question, however, is will any errors in the data affect resulting applications? In other words, what is the actual utility of SPOT DEMs given their known level of accuracy? Any use of the elevation data will contain all the errors of the DEM, but depending on the application, these errors may or may not have much affect on the derivative products. This paper evaluates the accuracy of a portion of a SPOT DEM relative to reference DEMs and the accuracy of derivative products, specifically slope and aspect, and demonstrates one application for the North Slope of Alaska.

UTILITY OF A DEM FOR ALASKA'S NORTH SLOPE

In much of Alaska, as in other remote area throughout the world, detailed topographic maps and/or stereoscopic aerial photographs are not available. For example, as of 1986, 1:25,000-scale maps of Alaska were in progress but not complete (Brooks

0099-1112/92/5806–815$03.00/0

and O'Brien, 1986). Having a ready source of topographic data for area where detailed data do not exist should be welcomed by geologists, ecologists, land use planners, and others. The digital form of the SPOT data enables them to be readily input to a GIS where large areas can be processed; digitization of elevations from maps or aerial photographs, in contrast, can be labor intensive for large areas.

DEM data in Alaska and similar areas have been used in land-use/land-cover mapping (Shasby and Carneggie, 1986; Fleming, 1980), vegetation mapping (Talbot and Markon 1986 and 1988), and in compensating for terrain effects on remotely sensed reflectances of snow (Dozier, 1989). They have also been used in correlation studies involving ecosystem variables such as vegetation cover and depth of thaw in a GIS (Evans *et al.*, 1989a, 1989b). Numerous investigators have noted how topography controls permafrost distribution (Brown, 1965; Bird, 1967; Brown and Pewe, 1973; Ferrians and Hobson, 1973; Dingman and Koutz, 1974; Morrissey *et al.*, 1986). The distribution of permafrost is critical in engineering planning and design as well as oil and gas exploration activities. Topography also controls vegetation distribution and growth as it is related to snow drifting, insolation, water availability, and depths of thaw (Bird, 1967; Viereck and Cleve, 1984; Evans *et al.*, 1989a, 1989b; Dingman and Koutz, 1974).

In this investigation, we present an example application of DEM data in an arctic ecosystem. Field data for depth to permafrost were collected in June and August 1987 at 110 locations, representing minimum and maximum thaw during the growing season. The difference between these is termed thaw thickness and represents the magnitude of the change in the active layer during that summer. As such, it is a measure of soil wetness and trafficability during the summer. Several years of field-collected thaw thicknesses should be used in a predictive model to estimate areas that are most likely to have poor trafficability during the growing season and, hence, an increased potential for soil disturbance. In this example, a single year was evaluated solely to demonstrate the utility of the technique. The technique involves correlating slope, aspect, surficial geology, and vegetation cover with thaw thickness. Thaw thickness estimates from the SPOT-derived and two map-derived DEM data sets are displayed to show how DEM accuracy affects such predictions.

The study site is located on the North Slope of Alaska near the Kuparuk River in the northern foothills of the Brooks Range, approximately 120 km southwest of Prudhoe Bay (Figure 1). The area (~25km²) is moderately diverse topographically, exhibiting large, relatively flat floodplain areas (0 to 5 percent slope) with upland slopes ranging from moderately sloping (6 to 10 percent slope) to sloping (11 to 31 percent slope). A moderate range of aspect (predominantly west-facing, with moderately large areas of flat, northeast, northwest, and southwest facing slopes) and moderate local relief (750 to 1000m) is also represented. There are few steep areas, and slopes in the area are generally long (500 to 1000 m) and relatively gentle (≤ 10 percent). This area has diverse vegetation types within a tussock/tundra type ecosystem (Walker *et al.*, 1987), which is one of the most widespread circumpolar ecosystems closely associated with Alaskan energy resources.

The study site is a designated U.S. Department of Energy (DOE) research area which has been intensively investigated by several universities under the auspices of DOE's R4D (Response, Resistance and Resilience to, and Recovery from, Disturbance in Arctic Ecosystems) program. The site provides an opportunity to test (within this small subset of the SPOT scenes) the suitability of SPOT as a data source for producing elevation and derivative data sets that may be useful in ecosystem investigations.

DATA SETS AND PROCESSING

The ability to "point" on-board sensors upon command at anywhere up to plus or minus 27 degrees off-nadir provides the possibility for acquiring relatively high-resolution stereoscopic data with SPOT over large geographic areas (Chevrel, 1981). The level 1A SPOT panchromatic, stereoscopic image pair used in this study was collected on 21 June 1987 at an incidence angle of 22.7° left of nadir and on 23 June 1987 at an incidence angle of 3.3° right of nadir (Figure 1) to approximately coincide with field data collection efforts. The SPOT data, collected only two days apart, were relatively cloud- and haze-free. Although the 23 June image was not collected at an ideal angle (i.e., not near the maximum incidence angle), the SPOT Image Corporation gave assurances that the difference between the angles of the two images of the pair (26°) was sufficient, though not optimum (i.e., approximately half of the maximum difference possible), to provide a base-to-height ratio (0.48), large enough to produce suitable stereoscopic data. Because it is difficult to acquire snow- and cloud-free images over the study area, this pair was used despite the low angle of the right image.

The DEM data, purchased from STX Corporation, was unpacked and subset using VICAR (Video Imaging, Communications, and Retrieval) to exclude data outside the study area, resulting in a 211,128-cell data set (each cell is 10m square). Every cell of this subset of the STX DEM was compared with reference data sets rather than with a limited number of check points. The subset was reformatted and processed with ERDAS (Earth Resources Data Analysis Systems) and in-house software.

Two reference data sets were used for comparison to the STX data. One was a 1:63,360-scale U.S. Geological Survey topographic map (Philip Smith Mountains (C-4), Alaska) with a 50-foot (15.24-m) contour interval. The other was a 1:6000-scale topographic map with a 5-metre contour interval; this was produced by North Pacific Aerial Surveys of Anchorage, Alaska from 1984 low-altitude aerial photographs using six control points. The contour lines of both were digitized, surfaced, and gridded to 10-m cells; elevations were recorded to the even metre in order to match the STX data. The DEM created from the 1:63,360-scale map was interpolated from digitized points using a search radius of 400m; a 200-m radius was used with the 1:6000-scale map. Both DEMs were created using a linearly decreasing weight for interpolated points as distance increases. Potential sources of errors in these reference data sets include interpolation errors in contouring the source maps and in DEM creation. Both maps were in the Universal Transverse Mercator (UTM) projection system as was the SPOT (STX) DEM. This allowed registration of the DEMs based on the UTM coordinates; equal grid sizes for all data sets allowed directly overlay. UTM coordinates of all data sets were assumed to be accurate to at least within the size of the cell (10m). The UTM coordinates used in digitizing were within at most a few metres of those on the original maps.

Residuals were computed as the differences (positive and negative) of each of the 211,128 cells between the reference data sets (1:6000-scale and 1:63,360-scale DEMs and slopes) and the test data set (STX DEM and slopes) using the ERDAS ALGEBRA program without rescaling the output file. An in-house program was used to compute average positive and negative errors (computed as the average amount of positive and negative errors for the whole data set divided by the total number of pixels) and root-mean-square errors. Aspects were evaluated with the ERDAS SUMMARY program which produces omission/commission data for each slope orientation by comparing the data sets on a cell-by-cell basis.

These methods of evaluating SPOT DEM accuracy provided a more complete check of this portion of the DEM (211,128 points) than checking only a limited number of selected points; the

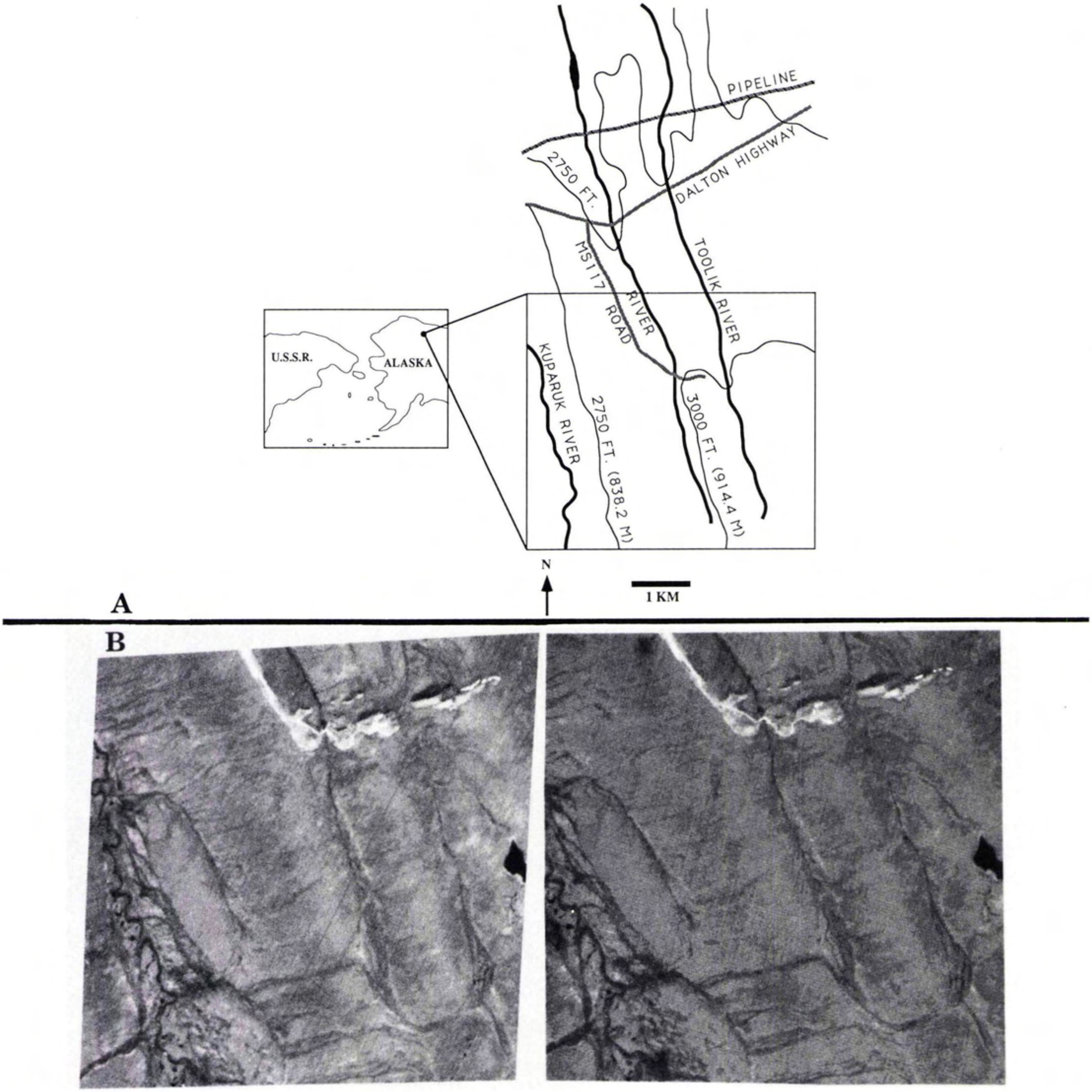

FIG. 1. Location (A) and subset of SPOT Level 1A (geometrically uncorrected/ungeoreferenced) panchromatic stereoscopic image pair (B), R4D study site near Toolik Lake, Alaska. The box on the map of the study site and the coverage of each image shows the approximate boundaries of the digital elevation model evaluated and displayed in subsequent figures.

SPOT DEM was evaluated at every point in the study area. This approach allows comparison of this portion of the SPOT DEM to other DEMs (the reference data sets) that might be used for ecosystem investigations in this area. In the North Slope of Alaska the best topographic map generally available for comparison is the 1:63,360-scale map. Because SPOT DEMs are reported to be more accurate than this, as previously discussed, a fair evaluation should use a reference data set that is at a higher resolution than SPOT. In the R4D study area this high resolution data need was met by the 1:6000-scale map. This latter map provided a very accurate DEM for evaluating a portion of the SPOT DEM at this study site.

RESULTS AND DISCUSSION

The STX DEM (Figure 2) was compared to two reference data sets, the 1:63,360-scale and the 1:6000-scale map-derived DEMs. These are referred to as the 15-m C.I. (contour interval) and the

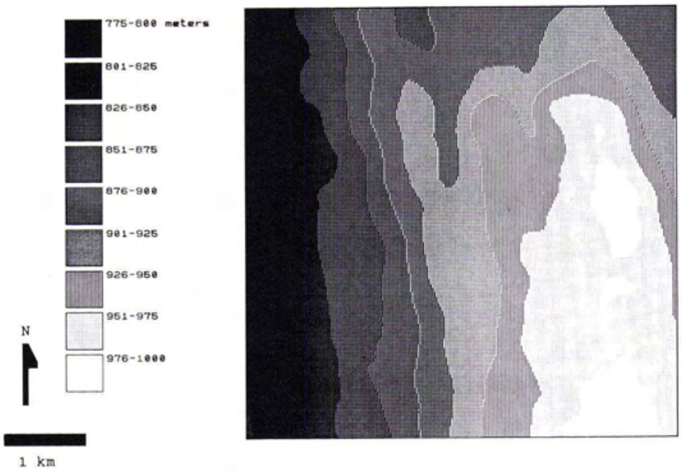

FIG. 2. Elevation class map derived from the SPOT image pair displayed in Figure 1.

TABLE 1. ELEVATION ERROR SUMMARY.

	STX vs.5mC.I.	STX vs.15mC.I.	15 vs. 5m C.I.
error range(m)=	-13 to +48	-10 to +35	-21 to +25
portion of data sets that:			
agree exactly(%)=	0.4	1.3	6.9
have negative errors(%)=	1.8	2.6	16.6
have positive errors(%)=	97.8	96.1	79.5
average error per pixel:			
negative(m)=	-0.1	-0.1	-0.8
positive(m)=	17.9	12.	6.6
root mean square error(m)=	19.3	13.7	9.
mean error(m)=	17.5	12.5	- 1.
std. dev. of error(m)=	18.5	13.5	14.1

5-m C.I. DEMs, respectively. The STX DEM was evaluated by measuring the difference between it and the two reference data sets. Any differences are referred to as errors in the STX DEM, although it is recognized that the reference data sets could actually be the data sets in error.

ELEVATIONS

Differences between the STX DEM and the 5-m C.I. and 15-m C.I. DEMs are summarized in Table 1 and Figures 3 and 4. The errors approximate normal distributions (Figure 4). The two reference data sets are obviously different; the 5-m C.I. data set is assumed to be most accurate due to the higher resolution (vertical and horizontal) of the original source map used to create this data set. Based on this assumption, the errors of the 15-m C.I. DEM are presented (Table 1 and Figure 4). The errors between the 15- and 5-m C.I. DEMs are slightly bimodal with modes at 2-m and 11-m error. This is interpreted to mean that, although many of the differences between these data sets are minimal (near 2-m error), there are still a substantial number of errors less than but approaching the contour interval of the 15-m C.I. DEM with a slightly greater number that are near the difference between the two contour intervals (10m).

The STX DEM is biased toward higher elevations (mostly positive errors) but is not systematically higher (i.e., elevations are not clearly offset by a constant) than either reference data set. The 15-m C.I. DEM is more biased toward higher elevations than is the 5-m C.I. DEM. This bias could be the result of a combination of systematic error and noise. Elevation errors are greatest in the STX DEM at two small, steep bedrock knobs in the northeastern part of the data set and lowest in flatter areas. The paucity of control points in remote area such as this could be responsible for the elevation errors. The STX DEM is in error by 3 to 4 contour intervals as compared to the 5-m C.I. DEM, and less than one contour interval as compared to the 15-m C.I. DEM. The difference between the 5-m C.I. and 15-m C.I. DEMs is important to note because many reference topographic maps may be no more accurate than the 15-m C.I. DEM. Although it is recognized that "elevation errors" could actually be registration/positional (x,y) errors, no independent source (e.g., additional survey points that are unambiguously identifiable on the SPOT image which were not already used in the STX DEM creation) was available to evaluate this.

SLOPE GRADIENTS

The STX DEM-derived slope was compared to the reference DEM-derived slopes. Slope gradients computed from the SPOT DEM approximated those from the 5-m and 15-m C.I.-derived DEMs, although small areas of steep slopes present on the ground were not present in the SPOT DEM slope data. Errors in the STX DEM-derived slopes (Figure 5), as compared with the 5-m and 15-m C.I. DEM-derived slopes, are summarized in Figure 6 and Table 2.

The slope gradients do not form a continuous range in values as is present on the ground; on the contrary, some classes are very frequent while other classes are empty (Figure 5). Slope errors reflect this also (Figure 6). This is especially true of slopes less than 10 percent. The SPOT DEM represents much more of the area as flat than really exists. The data also appear to be "stair-stepped" when in actuality there are subtle changes in slope gradient. Not surprisingly, Digital Terrain Data and Digital Elevation Models have been reported to be less accurate in areas of gentle slopes and complex relief than in steep areas (Carter, 1988). The vertical increment recorded for all DEMs in this study is 1m because that is the increment provided by STX. This increment has an impact on slopes computed in low gradient areas. Because the cells are 10-m square, any slope less than 10 percent (1m rise/10m run *100) in the principle directions or 7 percent (1m/(10m * $\sqrt{2}$) *100) in the diagonal directions will be calculated by the ERDAS SLOPE program as 0 percent or flat. This produces the "stair steps." There are at least three solutions to this artifact. One is to record the elevations to an accuracy of 0.1m (as the U.S. Geological Survey does for its large-scale DEMs). A second solution is to calculate the slope over a larger window (e.g., 10 cells length); this solution, however, may be problematic due to variability in elevations within such a large window. The third solution, similar to the second, is to enlarge the cell size. There is some justification for this approach. Peuker *et al.* (1976), for instance, report that elevation data should be gridded in DEMs to a grid cell size of 4.29 times the contour interval of the original source map for the DEM. As stated by Peuker *et al.* (1976), "Any grid spacing less than this would clearly imply redundancy, since it would appear of being capable of giving a precision higher than that of the source map (which is impossible)." Thus, for a contour interval of 5m (for the 1:6000-scale DEM), the cell should be 21.45m, and for a contour interval of 15.24m (for the 1:63,360-scale DEM), the cell should be 65.38m.

Because the grid cell size was thought to affect slope gradients and aspects as evidenced by the stair-stepped slopes, all DEMs were regridded. The STX DEM was gridded to 20-m and 70-m cells for comparison with the 5-m C.I. (gridded to 20m) and 15-m C.I. (gridded to 70m) data sets, respectively. Regridding was done using the ERDAS GCP, COORD2 and RECTIFY programs. Although the program was not used to rotate or translate the DEMs (as it is designed to do), these programs allow the DEMs to be interpolated (nearest neighbor method) and resampled.

The results of the comparison of the 20-m grid cell, 5-m C.I.

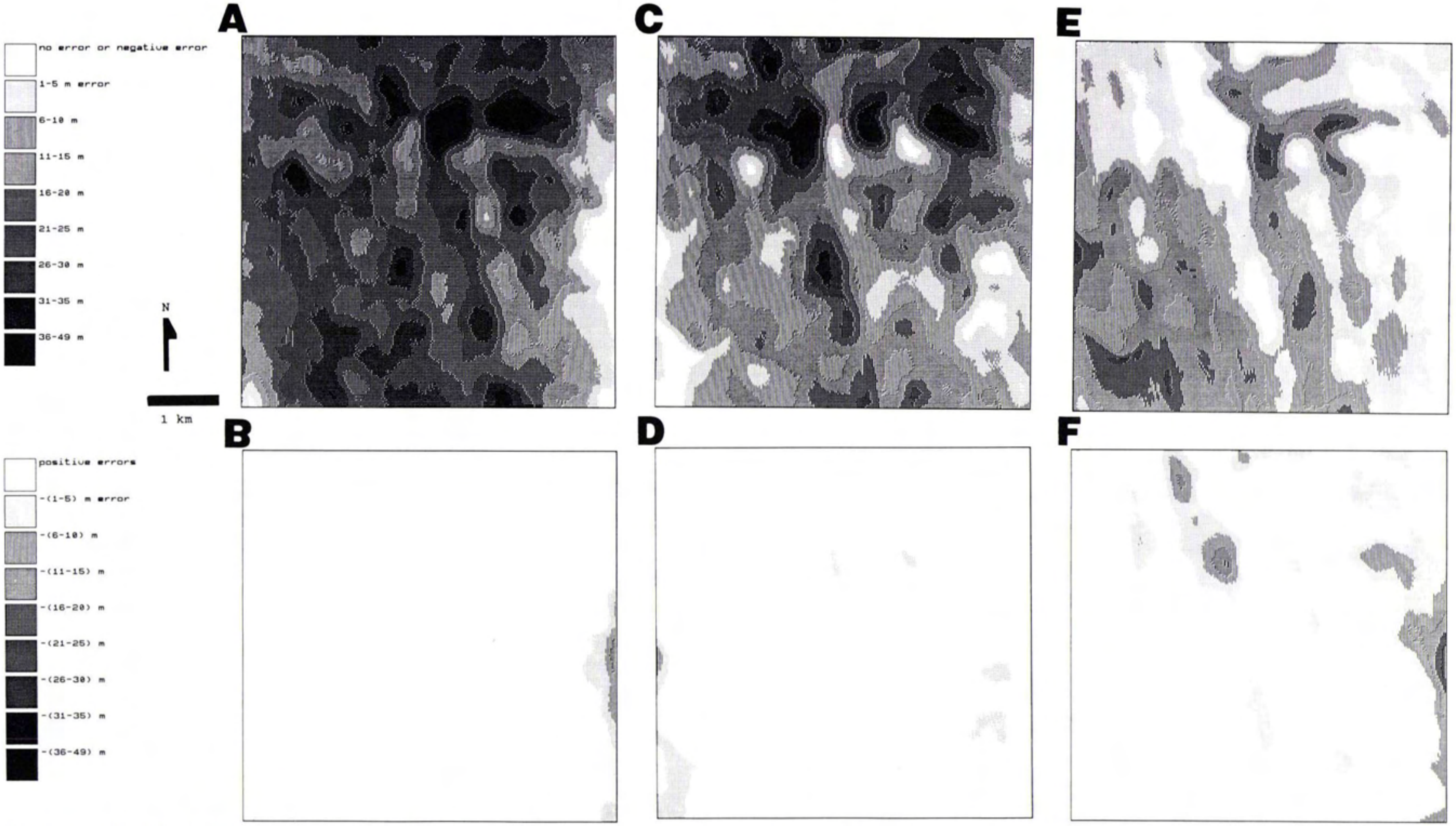

FIG. 3. Elevation differences: (a) positive errors, where the STX DEM is higher than the 5-m C.I. DEM; (b) negative errors, where the STX DEM is lower than the 5-m C.I. DEM; (c) positive errors, where the STX DEM is higher than the 15-m C.I. DEM; (d) negative errors, where the STX DEM is lower than the 15-m C.I. DEM; (e) positive errors, where the 15-m C.I. DEM is higher than the 5-m C.I. DEM; and (f) negative errors, where the 15-m C.I. DEM is lower than the 5-m C.I. DEM.

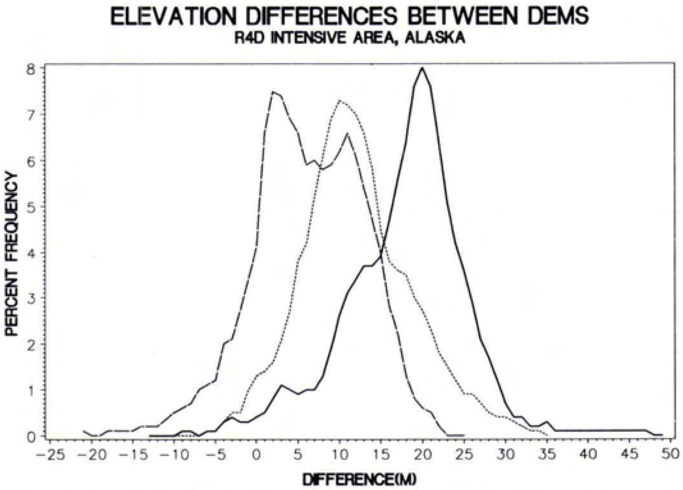

FIG. 4. Frequency distributions of elevation errors between STX, 5-m C.I., and 15-m C.I. DEMS. Solid line is the difference between the STX and the 5-m C.I. DEM (mean = 17.5m, standard deviation (s.d.) = 18.5m). Short dashed line is the difference between the STX and the 15-m C.I. DEM (mean = 12.5m, s.d. = 13.3m). Long dashed line is between the 5-m and 15-m C.I. DEMS (mean = −1m, s.d. = 14.1m).

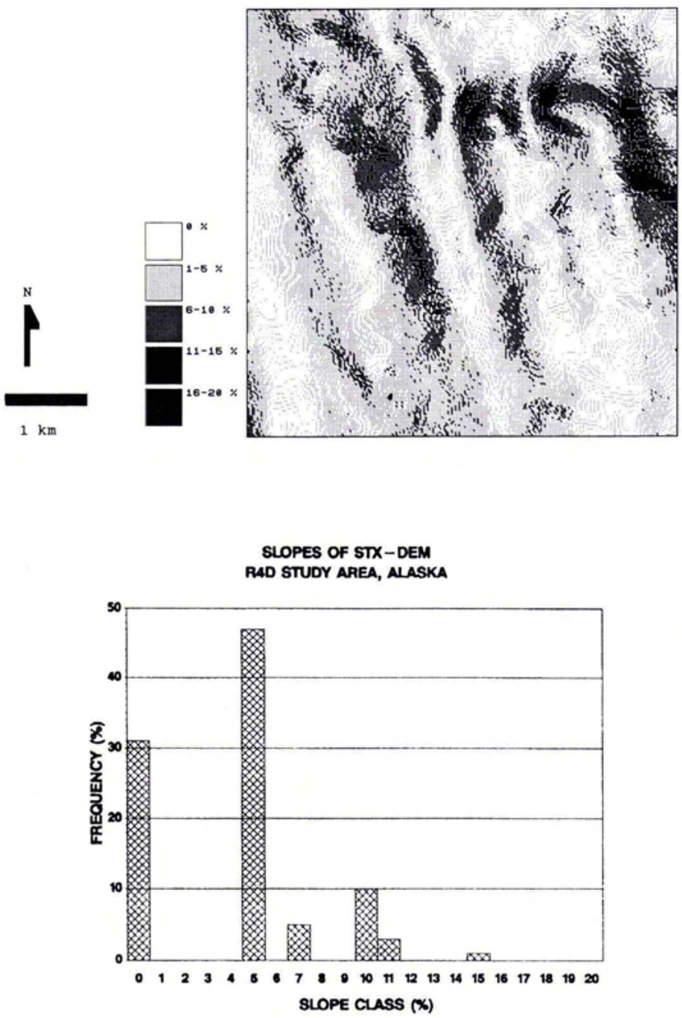

FIG. 5. Slope map and frequency distribution of the STX DEM-derived slope gradients.

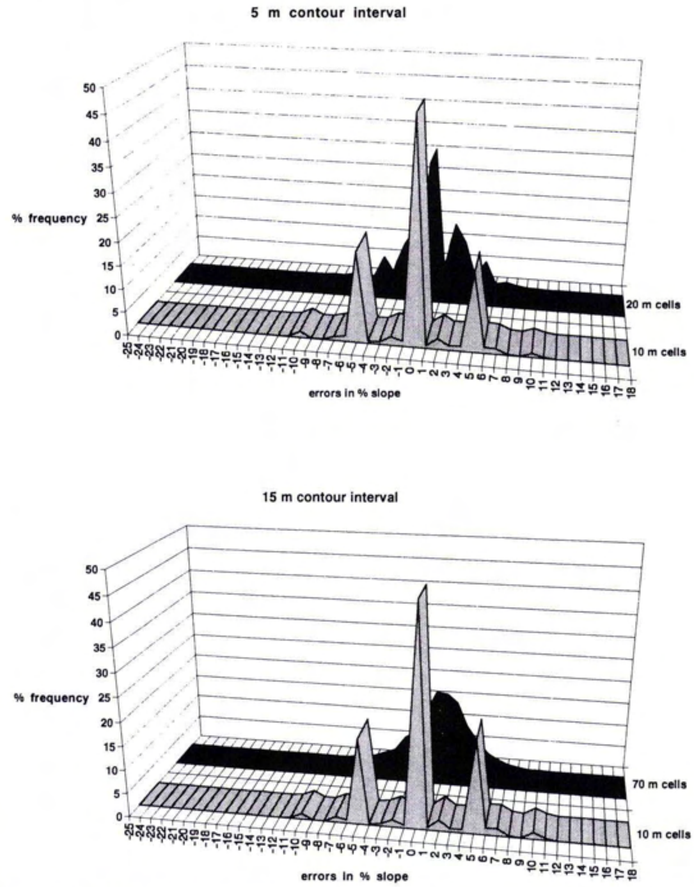

FIG. 6. Frequency distributions of slope errors between STX, 5-m C.I., and 15-m C.I. DEMS for 10-m and 20-m/70-m cells.

TABLE 2. SLOPE ERROR SUMMARY.

	STXvs.5mC.I. (10m cells)	STXvs.5mC.I. (20m cells)	STXvs.15mC.I. (10m cells)	STXvs.15mC.I. (70m cells)
error range(%)=	-18 to +18	-16 to +13	-25 to +15	-8 to +10
portion of data sets that:				
agree exactly(%)=	46.8	30.8	46.	16.6
have negative errors(%)=	27.4	32.1	24.5	30.8
have positive errors(%)=	25.8	37.1	29.5	52.6
average error per pixel:				
negative(%)=	-1.4	-1.	-1.3	-0.7
positive(%)=	1.3	1.2	1.5	1.4
root mean square error(%)=	3.9	3.	4.	2.7
mean error*(%)=	-0.9	-1.	-1.6	1.
std. dev. of error*(%)=	9.9	8.4	9.7	5.5

* Note: errors are not normally distributed except for the 70m cells (see Figure 6).

DEM-derived slopes with the 20-m grid cell, STX DEM-derived slopes and the results of the comparison of the 70-m grid cell, 15-m C.I. DEM-derived slopes with the 70-m grid cell, STX DEM-derived slopes are summarized in Figure 6 and Table 2. The STX DEM-derived slopes generally bracket the reference slopes. Both positive and negative slope errors are generally greatest in the steepest areas and lowest in the flatter areas. Average per-pixel errors are quite low (near 1 percent) and would have little impact on most uses of the data. Exceptions to this are in local areas of high slope (e.g., near the bedrock knobs). Because elevations are in greatest error near the steep areas (bedrock knobs) and least near the flat areas, it follows that slopes would be in greatest and least error, respectively, at these locations. Using

TABLE 3. CONFUSION MATRIX OF 10-M CELL-SIZED ASPECTS: (A) AGREEMENT BETWEEN STX AND 5-M C.I. DEM; AND (B) AGREEMENT BETWEEN STX AND 15-M C.I. DEM. NUMBERS IN PARENTHESES ARE THE SUM OF THE NUMBERS (ACROSS THE ROW) IN THE SHADED AREA, I.E., THEY REPRESENT THE AGREEMENT PLUS OR MINUS ONE CLASS.

A

	East	Northeast	North	Northwest	West	Southwest	South	Southeast	Flat
East	44.09(74.32)	28.99	4.49	4.14	2.70	0.33	0.00	1.24	14.01
Northeast	32.27	43.94(82.47)	6.26	4.12	1.95	0.20	0.01	0.40	10.85
North	9.03	28.44	21.75(65.95)	15.76	8.30	0.83	0.05	0.97	14.87
Northwest	0.73	3.33	11.92	29.15(71.73)	30.66	7.43	0.68	0.89	15.21
West	0.21	0.25	0.99	10.90	64.83(91.52)	15.79	0.47	0.46	6.10
Southwest	0.63	0.72	0.84	9.34	61.54	17.58(79.95)	0.83	1.01	7.52
South	22.45	9.44	5.10	12.50	10.20	3.32	3.83(19.91)	12.76	20.41
Southeast	62.44	9.87	1.83	2.11	0.35	0.70	1.90	11.49(75.83)	9.30
Flat	8.63	11.66	6.93	16.80	20.14	3.86	1.01	2.32	28.65

B

	East	Northeast	North	Northwest	West	Southwest	South	Southeast	Flat
East	52.73(80.72	25.04	2.49	2.32	1.01	0.10	0.42	2.95	12.95
Northeast	33.20	49.48(87.32)	4.64	1.69	0.95	0.09	0.05	1.05	8.84
North	7.44	30.52	28.25(74.32)	15.55	5.27	1.55	0.15	0.94	10.32
Northwest	2.50	3.20	7.55	25.50(67.63)	34.58	12.08	0.92	1.23	12.43
West	0.62	0.73	1.02	10.92	64.12(89.92)	14.88	0.29	0.31	7.10
Southwest	0.89	1.24	1.10	8.98	63.78	16.06(80.48)	0.64	0.29	7.02
South	4.00	1.00	9.00	18.00	11.00	1.00	14.00(32.00)	17.00	25.00
Southeast	22.08	26.77	4.70	4.20	1.10	1.10	10.39	10.99(40.06)	18.68
Flat	6.75	11.49	7.81	17.44	22.81	4.81	0.83	1.68	26.37

TABLE 4. CONFUSION MATRIX OF 20-M AND 70-M CELL-SIZED ASPECTS: (A) 20-M CELL-SIZED DATA — AGREEMENT BETWEEN STX AND 5-M C.I. DEM; (B) 70-M CELL-SIZED DATA — AGREEMENT BETWEEN STX AND 15-M C.I. DEM.

A

	East	Northeast	North	Northwest	West	Southwest	South	Southeast	Flat
East	52.39(79.48)	25.88	6.45	5.86	3.94	0.42	0.00	1.21	3.85
Northeast	28.11	49.78(86.61)	8.72	5.55	2.64	0.25	0.04	0.38	4.53
North	8.20	30.62	23.74(73.67)	19.31	11.76	0.63	0.00	0.72	5.03
Northwest	1.25	3.91	12.97	33.82(81.89)	35.10	6.34	0.87	1.27	4.48
West	0.37	0.43	1.27	10.77	70.04(94.87)	14.06	0.61	0.80	1.63
Southwest	1.94	2.00	1.66	12.65	58.39	16.95(76.83)	1.49	1.94	2.98
South	32.59	16.30	7.41	14.07	8.89	0.74	0.74(18.52)	17.04	2.22
Southeast	69.35	11.41	2.01	0.89	0.00	0.00	2.68	11.86(83.89)	1.79
Flat	9.15	13.20	9.80	24.50	22.72	3.44	2.15	2.43	12.60

B

	East	Northeast	North	Northwest	West	Southwest	South	Southeast	Flat
East	53.92(78.83)	21.16	7.85	9.56	3.41	0.00	0.34	3.75	0.00
Northeast	22.70	60.22(89.89)	6.97	4.27	4.04	0.00	0.00	1.35	0.45
North	7.27	30.10	35.64(82.00)	16.26	9.00	0.69	0.35	0.35	0.35
Northwest	3.63	3.42	7.69	32.91(78.42)	37.82	9.83	1.50	3.21	0.00
West	1.13	1.44	2.05	9.62	76.06(94.52)	8.84	0.44	0.35	0.09
Southwest	0.70	0.00	1.41	7.04	75.35	12.68(90.85)	2.82	0.00	0.00
South	0.00	33.33	0.00	33.33	0.00	0.00	33.33(33.33)	0.00	0.00
Southeast	18.75	18.75	18.75	0.00	0.00	0.00	25.00	18.75(62.50)	0.00
Flat	0.00	7.59	17.72	41.77	32.91	0.00	0.00	0.00	0.00

a larger cell size makes error distributions more normal and decreases the error range, average per-pixel errors, and RMS errors, but does not improve the portion of the data sets that agree exactly.

SLOPE ASPECTS

The 10-m, 20-m, and 70-m cell STX-DEM-derived aspects were evaluated against the aspects derived from the reference data sets by comparing the orientations of all pixels. Table 3 contains the confusion matrices showing the commission-omission errors and the degree of agreement between the 10-m data sets; Table 4 contains confusion matrices for the degree of agreement between the 20-m data sets and the 70-m data sets. The greatest agreement is generally with westerly aspects and the least with southerly aspects. The data sets are composed of predominantly westerly aspects with few southerly aspects (Figure 7). In other words, the most prevalent slope direction is very accurately represented in the STX DEM-derived aspects, while the least frequent aspects are poorly reproduced in the STX aspects. Overall, the 20-m and 70-m data sets produce better matches with each other than the 10-m data sets, although the results are similar regardless of cell size. The exact slope orientation is not well matched by the STX data except for west-facing slopes in some cases. The general orientation, however, is well matched by the STX data for all orientations except the rarely present aspects in some cases.

THAW LAYER THICKNESS

One application of DEM data is to integrate them into a GIS and use them as a data layer in a predictive model. An example

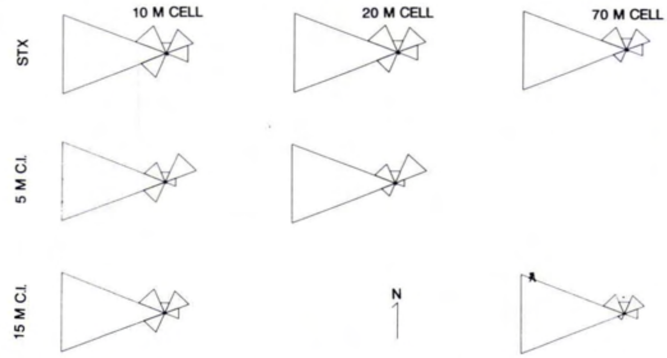

FIG. 7. Rose diagrams of slope aspect frequencies. Columns indicate the cell sizes and rows indicate the DEM sources from which aspects were computed.

of this type of application is demonstrated here with a simple model that predicts thaw layer thickness. The model uses as input a terrain unit layer (surficial geologic units, slope, and aspect) and a vegetation layer. The terrain unit layer has 252 classes made up of combinations of twelve geologic units, three slope classes (1 to 7 percent, 8 to 15 percent, > 15 percent), and nine aspect classes (the four cardinal and four diagonal directions and undefined or flat); some combinations are not present and thus are not classified. The vegetation layer has 19 classes based on species combinations that are related to surface moisture availability. The model assigns a thaw layer thickness to each 10-m pixel based on correlations between surface measurements of thaw layer thickness and terrain units and vegetation combinations.

All three data sets predicted a 50- to 100-cm thaw layer thickness for a majority of the areas with a moderate area of 0 to 50-cm thaw layer thickness (Figure 8). In all data sets these areas are generally in the same locations. If the 5-m C.I. DEM is treated as the data set that would produce the most accurate predictions of thaw layer thickness, then the STX DEM is more accurate than the 15-m C.I. DEM. The 15-m C.I. DEM overpredicts small areas of 200- to 250-cm thaw thickness, i.e., the most active areas. Further research is needed to evaluate if the model predictions represent ground conditions.

SUMMARY AND CONCLUSIONS

SPOT can produce relatively high-quality DEMs at large scales for large areas, even under less than optimum acquisition angles (3.3° off nadir for the right image) and, hence, a low base-to-height ratio (0.48). This SPOT DEM correctly depicts the long, gently sloping topography of an area on the North Slope of Alaska. The elevations are biased 12 to 18m higher in the SPOT DEM than the two reference DEMs, but errors are not systematic.

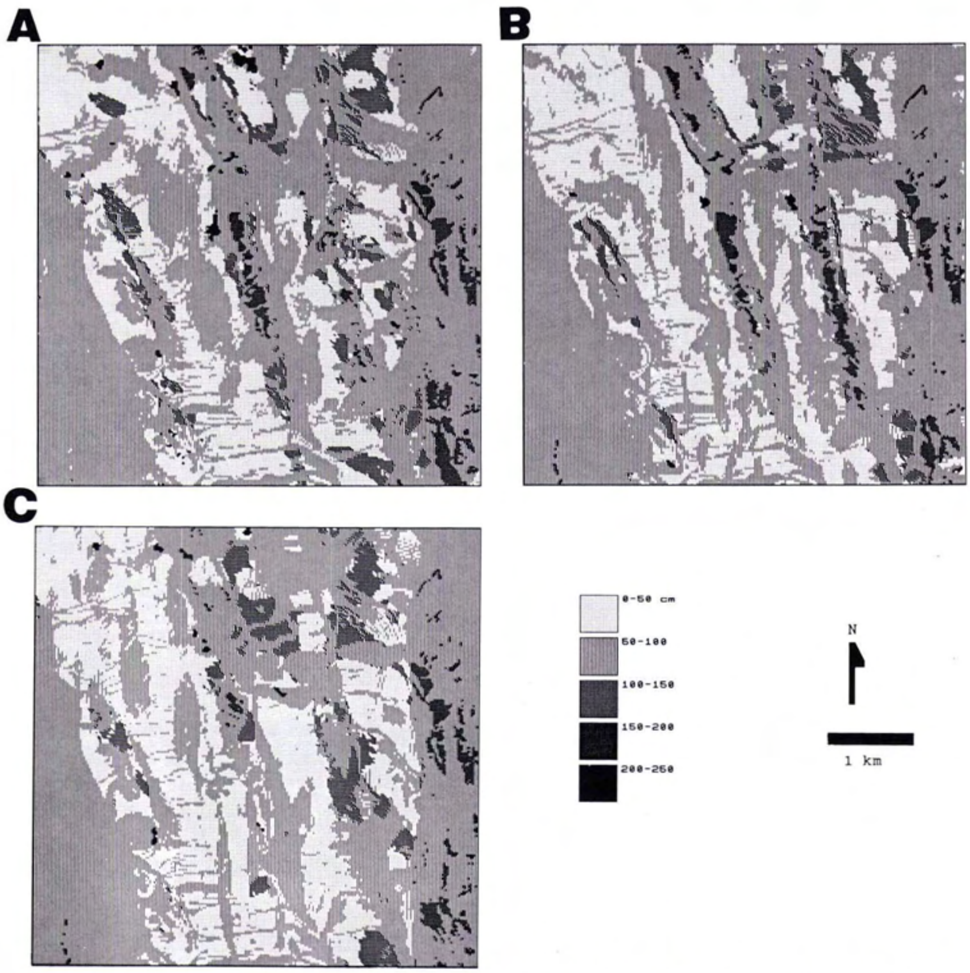

FIG. 8. Predictions of thaw layer thickness: (a) from STX DEM-derived slopes and aspects; (b) from 5-m C.I. DEM-derived slopes and aspects; and (c) from 15-m C.I. DEM-derived slopes and aspects.

Elevation errors at specific points (e.g., small, steep areas) can be large but these areas are of very limited areal extent. Slope gradients computed from the SPOT DEM average ± 1.5 percent as compared to the two reference DEM-derived slopes. Errors in slopes, as in the elevations, can be great in some areas (e.g., steep areas) and are lowest over the majority of this site which has predominatly low slopes (<5 percent). Slope aspects computed from the SPOT and reference DEMs are predominantly west-facing slopes. SPOT-derived aspects relatively accurately reproduce the west-facing slopes but poorly reproduce the least prevalent aspects.

For most of the world where other DEM data are unavailable, SPOT DEMs can provide data to enable natural resource researchers to investigate relationships between topography and such variables as land use, terrain effects on remotely sensed data, and vegetation cover. In arctic ecosystems topography controls snow drifting, insolation, water availability, and locations of thaw; these, in turn, affect vegetation growth, trafficability, and the potential for disturbance among other ecosystem variables. A SPOT DEM was used with other digital data to predict thaw layer thickness as a demonstration of the potential utility for such data. Although data quality can be limited by snow and cloud cover, SPOT DEMs still have great potential for extending landform geometry investigations into areas such as the North Slope of Alaska, where large-scale topographic maps do not currently exist.

ACKNOWLEDGMENTS

This project was funded by the U.S. Department of Energy, Office of Health and Environmental Research, Ecological Research Division. Dr. Frank Wobber of U.S.D.O.E. is gratefully acknowledged. Figure 1 contains portions of two SPOT images (Copyright SPOT Image Corporation 1987). STX Remote Sensing Services of Lanham, Maryland supplied the digital elevation data which they derived from the SPOT stereoscopic images. Doug Miller of ORSER at The Pennsylvania State University helped with preprocessing on the MicroVAX. Celeste Jarvis of ORSER stimulated discussions on this topic, and Rick Day and Les Lanyon of the Agronomy Department at The Pennsylvania State University provided helpful comments regarding an earlier version of the manuscript.

REFERENCES

Arai, K., N. Fujimoto, H. Sato, and S. Koizumi, 1988. Terrain Height Estimation Using a HRV Stereo Pair. *Intl. Archives of Photogram. and Remote Sensing*. Vol. 27, Part B2, Commission II, pp. 20–28.

Bird, J. B., 1967. *The Physiography of Arctic Canada:* The John Hopkins Press, Baltimore, Maryland, pp. 33–45.

Brockelbank, D. C., and Tam, A. P., 1991. Stereo Elevation Determination Techniques for SPOT Imagery. *Photogrammetric Engineering & Remote Sensing*. Vol. 57, No. 8, pp. 1065–1073.

Brooks, P. D., and T. J. O'Brien, 1986. The Evolving Alaska Mapping Program. *Photogrammetric Engineering & Remote Sensing*. Vol. 52, No. 6, pp. 769–777.

Brown, R. J. E., 1965. Some Observations on the Influence of Climatic and Terrain Features on Permafrost at Norman Wells, N.W.T., Canada. *Canadian Journal of Earth Sciences*, Vol. 2, pp. 15–31.

Brown, R. J. E., and T. C. Pewe, 1973. Distribution of Permafrost in North America and its Relationship to the Environment: A Review, 1963–1973. *Permafrost, 2nd Intl. Conf.*: National Academy of Sciences, Washington, D.C., pp. 71–100.

Carter, J. R., 1988. Digital Representations of Topographic Surfaces. *Photogrammetric Engineering & Remote Sensing*, Vol. 54, No. 11, pp. 1577–1580.

Chen, L.-C., L.-H Lee, and S.-C. Lee, 1988. DTM Generation Using SPOT Digital Data. *Intl. Archives of Photogram. and Remote Sensing*, Vol. 27, Part B3, Commission III, pp. 100–109.

Chevrel, M., M. Courtois, and G. Weill, 1981. The SPOT Satellite Remote Sensing Mission. *Photogrammetric Engineering & Remote Sensing*, Vol. 47, No. 8, pp. 1163–1171.

Cooper, P. R., D. E. Friedman, and S. A. Wood, 1987. The Automatic Generation of Digital Terrain Models from Satellite Images by Stereo. *Acta Astronautica*, Vol. 15, No. 3, pp. 171–180.

Day, J., and J.-P. Muller, 1989. Digital Elevation Model Production by Stereo-Matching SPOT Image - Pairs: A Comparison of Algorithms. *Image and Vision Computing*, Vol. 7, No. 2, pp. 95–101.

Dingman, S. L., and F. R. Koutz, 1974. Relations Among Vegetation, Permafrost, and Potential Insolation in Central Alaska. *Arctic and Alpine Research*, Vol. 6, No. 1, pp. 37–42.

Dowman, I. J., 1988. The Prospects for Topographic Mapping Using SPOT Data: *SPOT 1 Image Utilization Assessment, Results:* Cepadues-Editions, Toulouse, France: pp. 1163–1172.

Dozier, J., 1989. Spectral Signature of Alpine Snow Cover from the Landsat Thematic Mapper: *Remote Sensing of Environment*, Vol. 28, pp. 9–22.

ERDAS, Inc., 1987. *ERDAS PC and PC-kit Image Processing System*, Earth Resources Data Analysis System, Atlanta, Georgia.

Evans, B. M., G. W. Petersen, and K. F. Connors, 1989a. *Hypothesis Testing of Watershed/Landscape Dynamics in Northern Alaska Using Digital Analysis*, ER8907. Environmental Resources Research Institute, University Park, Pennsylvania, 53 p. + appendices.

Evans, B. M., D. A. Walker, C. A. Benson, E. A. Nordstrand, and G. W. Petersen, 1989b. Spatial Interrelationships Between Terrain, Snow Distribution and Vegetation Patterns at an Arctic Foothills Site in Alaska. *Holarctic Ecology*, Vol. 12, No. 3, pp. 270–278.

Ferrians, O. J., and G. D. Hobson, 1973. Mapping and Predicting Permafrost in North America, A Review, 1963–1973. *Permafrost, 2nd Intl. Conf.*: National Academy of Sciences, Washington, D.C., pp. 479–498.

Fleming, M. D., 1988. An Integrated Approach for Automated Cover-Type Mapping of Large Inaccessible Areas in Alaska, *Photogrammetric Engineering & Remote Sensing*, Vol. 54, No. 3, pp. 357–362.

Forster, B. C., J. C. Trinder, D. Carroll, R. Farrington, and L. Kwoh, 1988. Mapping and Urban Multi-Experimental Assessment of SPOT - Mapping Results. *SPOT 1 Image Utilization, Assessment, Results*: Cepadues-Editions, Toulouse, France: pp. 1289–1295.

Fukushima, Y., 1988. Generation of DTM Using SPOT Image Near Mt. Fuji by Digital Image Correlation. *Intl. Archives of Photogram. and Remote Sensing*, Vol. 27, Part B3, Commission III, pp. 225–234.

Gugan, D. J., and I. J. Dowman, 1988a. Topographic mapping from SPOT Imagery. *Photogrammetric Engineering & Remote Sensing*, Vol. 54, No. 10, pp. 1409–1414.

———, 1988b. Accuracy & Completeness of Topographic mapping from SPOT Imagery. *Photogrammetric Record*, Vol. 12, No. 72, pp. 787–796.

Hanaizumi, H., T. Hibino, and S. Fujimura, 1990. An Automatic Method for Terrain Height Estimation from SPOT Stereo Pair Images Using Correlation Between Epipola Lines. *Remote Sensing for the Nineties, 10th Annual International Geoscience and Remote Sensing Symposium*, Vol. III, pp. 1959–1962.

Hartley, W. S., 1988. Topographic Mapping with SPOT 1 Data. A Practical Approach by the Ordnance Survey: *SPOT 1 Image Utilization, Assessment, Result*: Cepadues-Editions, Toulouse, France: pp. 1245–1265.

Koizhmi, S., K. Ayabe, H. Sato, K. Arai, S. Yamamoto, T. Nakazawa, K. Tachi, N. Fujimoto, K. Tsuchiya, and R. Tateishi, 1988. Studies on System Performance of SPOT (Space and Ground Segments): *SPOT 1 Image Utilization, Assessment, Results*: Cepadues-Editions, Toulouse, France: pp. 1305–1313.

Ley, R. G., 1988. Some Aspects of Height Extraction from SPOT Imagery. *Photogrammetric Record*, Vol. 12, No. 72, pp. 823–832.

Millot, M., and P. N. Pascand, 1988. Automatic Production of Orthophoto Using SPOT Images: *SPOT 1 Image, Utilization, Assessment, Results*: Cepadues-Editions, Toulouse, France: pp. 1325–1330.

Morrissey, L. A., L. L. Strong, and D. H. Card, 1986. Mapping Permafrost in the Boreal Forest with Thematic Mapper Satellite Data. *Photogrammetric Engineering & Remote Sensing*, Vol. 52, No. 9, pp. 1513–1520.

Peuker, T. K., R. J. Fowler, J. J. Little, and D. M. Mark, 1976. *Digital Representation of Three-Deminsional Surfaces by Triangulated Irregular Networks (TIN)*, Technical Report No. 10, Office of Naval Research, U.S.A.

Priebbenow, R., and E. Clerici, 1988. Cartographic Applications of SPOT Imagery: *SPOT 1 Image Utilization, Assessment, Results*: Cepadues-Editions, Toulouse, France: pp. 1189–1203.

Rodriguez, V., P. Gigord, A. C. de Gaujac, P. Munier, and G. Begni, 1988. Evaluation of the Stereoscopic Accuracy of the SPOT Satellite. *Photogrammetric Engineering & Remote Sensing*, Vol. 54, No. 2, pp. 217–221.

Rosenholm, D., 1988. Multi-point Matching Along Vertical Lines in SPOT Images. *International Journal of Remote Sensing*, Vol. 9, Nos. 9 and 10, pp. 1687–1703.

Shasby, M., and D. Carneggie, 1986. Vegetation and Terrain Mapping in Alaska Using Landsat MSS and Digital Terrain Data. *Photogrammetric Engineering & Remote Sensing*, Vol. 52, No. 6, pp. 779–786.

Simard, R., G. Rochon, and A. Leclerc, 1988. Mapping with Spot Imagery and Integrated Data Sets. *Intl. Archives of Photogram. and Remote Sensing*, Vol. 27, Part B11, Commissions I–VII, pp. IV-440–IV–449.

Swann, R., D. Kauffman, and B. Sharpe, 1988. Results of Automated Digital Elevation Model Generation from SPOT Satellite Data. *Intl. Archives of Photogram. and Remote Sensing*, Vol. 27, Part B2, Commission II, pp. 434–440.

Talbot, S. S., and C. J. Markon, 1986. Vegetation Mapping of Nowitna National Wildlife Refugee, Alaska, Using Landsat MSS Digital Data. *Photogrammetric Engineering & Remote Sensing*, Vol. 52, No. 6, pp. 791–799.

———, 1988. Intermediate-Scale Vegetation Mapping of Innoko National Wildlife Refuge, Alaska Using Landsat MSS Digital Data. *Photogrammetric Engineering & Remote Sensing*, Vol. 54, No. 3, pp. 377–383.

Theodossiou, E. I., and I. J. Dowman, 1990. Heighting Accuracy of SPOT. *Photogrammetric Engineering & Remote Sensing*, Vol. 56, No. 12, pp. 1643–1649.

Thormodsgard, J. M., and J. W. Feuguay, 1988. Layer Scale Image Mapping with SPOT:; *SPOT 1 Image Utilization, Assessment, Results*: Cepadues-Editions, Toulouse, France: pp. 1272–1279.

Veenstra, C., and C. Master, 1988. Assessment of SPOT Imagery for Topographic Revision and Vegetation Mapping: *SPOT 1 Image Utilization, Assessment, Results*: Cepadues-Editions, Toulouse, France: pp. 1229–1234.

Viereck, L. A., and K. vanCleve, 1984. Some Aspects of Vegetation and Temperature Relationships in the Alaska Taiga, *The Potential Effects of Carbon Dioxide-Induced Climatic Changes in Alaska* (J. H. McBeath, G. P. Juday, G. Weller, and M. Murray, editors), Misc. Pub. 83-1: School of Agric. and Land Resources Mgmt., Univ. of Alaska, Fairbanks, pp. 129–142.

Vincent, R. K., M. A. True, and P. K. Pleitner, 1988. Automatic Extraction of High Resolution Elevation Data from SPOT Stereo Images: *SPOT 1 Image Utilization, Assessment, Results*: Cepadues-Editions, Toulouse, France: pp. 1339–1345.

Walker, D. A., P. J. Webber, N. D. Lederer, and M. D. Walker, 1987. *Terrain and Vegetation of The Department of Energy R4D Research Site, Imnavait Creek, Alaska: I. Classification and Mapping*, Draft Manuscript: Plant Ecology Laboratory, Institute of Arctic and Alpine Research, Univ. of Colorado, Boulder, Colorado: 68 p.

Westin, T., 1988. Production of Satellite Image Maps Based on SPOT Data: *SPOT-1 Image Utilization, Assessment, Results*: Cepadues-Editions, Toulouse, France: pp. 1357–1363.

(Received 1 March 1991; revised and accepted 29 October 1991)